Available online at www.sciencedirect.com
ScienceDirect
Journal of Magnetic Resonance 188 (2007) 322–329
JMR Journal of Magnetic Resonance
www.elsevier.com/locate/jmr

# Diffusive diffraction measurements in porous media: Effect of structural disorder and internal magnetic field gradients

Jean-François Kuntz [a], Pascal Palmas [a,*], Daniel Canet [b]

[a] Commissariat à l'Energie Atomique, Le Ripault, BP 16 37260 Monts (Tours), France
[b] Méthodologie RMN, UMR7565 CNRS-UHP, Université Henri Poincaré, BP 239 54506 Vandoeuvre-lès-Nancy Cedex, France

Received 1 June 2007; revised 13 August 2007
Available online 19 August 2007

**Abstract**

Pulsed Field Gradient NMR (PFG-NMR) method used to measure the self-diffusion coefficient of liquids can also be exploited to probe the local geometry of porous media. In most practical cases, the measured diffusion attenuation is generally Gaussian and can be interpreted in terms of an apparent diffusion coefficient. Using well chosen experimental conditions, a so called "diffusive diffraction" phenomenon can be observed in the diffusion curve with a specific shape and maxima location characteristic of the system local dimensions. In this paper we investigate this phenomenon by presenting new experimental results obtained on several porous model systems of packed sphere particles. Using different experimental approaches, the diffusion pattern could be finely observed and interpreted in the context of the pore hopping model formalism. Different calibrated systems of polystyrene and glass spheres with known mean diameter and polydispersity were used to investigate specifically the influence of structural heterogeneity and local internal gradients. Structural data obtained in that way were found in close agreement with laser diffraction granulometry measurement and Scanning Emission Microscopy.


*Keywords:* NMR; Diffusion; Diffraction; Structural heterogeneity; Internal gradient

## 1. Introduction

Magnetic field gradients have, over the past 20 years, been the basis for the development of a number of NMR pulse sequences for imaging and diffusion measurements. Most of these methods have been used to investigate the structure and transport properties in porous media embedded with a fluid. The extent of porous media is very wide: sandstone, other rocks, catalysts, biological tissues, or polymers and glass beads are typical examples of such materials and are generally important in industrial applications in various domains like oil production, food science and pharmaceutical engineering. The spatial resolution of Magnetic Resonance Imaging has an upper limit which is given by the voxel (about 1000 $\mu m^3$ with standard equipment) and more fundamentally by the NMR linewidth [1]. In practice, information about the pore scale can be obtained by this method only when cavity dimensions are higher than a few dozen micrometers. Even when the resolution is not sufficient, imaging can still yield macroscopic information on the distribution or diffusion of fluids inside a material, for instance, from images contrasted by relaxation times. A second approach, i.e., measurement of molecular self-diffusion, is another way of extracting structural features by probing the restriction of molecular displacements in a confined fluid [2]. The use of Pulsed Gradient Spin Echo NMR (PGSE NMR) to measure the influence of boundaries on a diffusing molecule was first demonstrated by Tanner and Stejskal [3]. Subsequently the usefulness of such a technique in the determination of pore size, tortuosity, and surface to volume ratio (S/V) was fully recognized [4–6]. The main idea of these studies is the

* Corresponding author. Fax: +02 47 34 51 48.
*E-mail address:* pascal.palmas@cea.fr (P. Palmas).

1090-7807/$ - see front matter © 2007 Elsevier Inc. All rights reserved.
doi:10.1016/j.jmr.2007.08.009

determination of an effective diffusion coefficient and the exploitation of its variation as a function of the diffusion interval Δ which separates the encoding and decoding gradient pulses. This approach relies on the assumption that a Gaussian distribution of molecular displacements still holds even in the restricted diffusion case. This is a first approximation, which is generally valid for most real heterogeneous materials but which, formally, depends on experimental conditions, i.e. pulse sequence, gradient intensity and duration, diffusion interval.

However, it has been shown experimentally that a deviation from this Gaussian form can occur under some circumstances, leading to the so-called ''diffusive diffraction'' effect in the *q-space* representation [7]. The pattern of the diffusion curve potentially gives access to the size and shape of the confined geometry. Many systems have been theoretically and experimentally described, including rectangular structures [8], plates [9], and cylinders [10]. The so-called ''hopping model'' was proposed to account for systems made up of interconnected boxes [11]. Applications of this approach for the interpretation of experimental data were reported for three different kinds of samples: beads of mono-disperse spherical polymer particles, water/oil emulsions and red blood cell suspensions [12–14]. All theses systems are characterized by a high level of organisation and homogeneity of pore surfaces and connections. Conversely, the observation of the diffusive diffraction pattern on a real porous material is much more difficult and was reported only recently [15]. This is due to both the structural heterogeneity (complex pore shape and connections and a large distribution of pore dimensions) and local field gradients produced by anisotropy susceptibility differences at interfaces. Both effects spread out the fine structure and damp the diffusion oscillations precluding the observation of any specific diffraction pattern.

In this paper, we shall provide a further insight into the diffusive diffraction phenomenon by presenting new experimental results on different samples of closely packed calibrated spherical particles embedded with a liquid. In a first part the diffraction effect is shown in the case of beads of polystyrene spheres similar to those used previously by Callaghan et al. [12] but with lower particle diameters (≈16 μm in Callaghan's work vs. ≈9 μm here). Starting with a first fraction possessing a weak size distribution ($\sigma < 15\%$; we define the dispersion $\sigma$ as the ratio, expressed in percentage, of the diameter standard deviation over the mean diameter) the diffraction phenomenon could be finely observed and used to validate the different NMR sequences. By controlling the particles size distribution, such a system provides the opportunity to evaluate the influence of structural heterogeneity on the diffraction effect. Taking advantage of this property we studied a second sample involving a higher poly-dispersity ($\sigma \approx 24\%$). In such a system the highly regular porous structure, the smooth surfaces, and the low magnetic susceptibility difference between polystyrene and water produce only weak internal magnetic field gradients (background gradients). To specifically investigate the effect of these local gradients we turned finally to another system of poly-disperse glass spheres (≈31 μm in diameter) as the magnetic susceptibility difference is much higher at the glass/water interface. The aim of the present work is to investigate the ability to observe the diffraction pattern in such a sample through three different experimental approaches. First, the bipolar version of the Stimulated Echo Pulse Field Gradient experiment (hereafter denoted PFGSTE_BP), where a pair of pulses of inverse polarity separated by a π pulse is introduced instead of the single gradient pulse used in the original experiment [16]. Second, the further improved version of the sequence proposed by Latour et al. (hereafter denoted cycled STE_BP), which uses a train of shorter gradient pulses of alternating sign, separated by RF π pulses [17]; and, thirdly, the approach which uses the gradient of the radio-frequency magnetic field $B_1$ [18]. The results obtained here on model systems of packed spheres are compared with those already reported for a real polymer material [15] with a special attention to internal gradient effects.

## 2. Results and discussion

### 2.1. Polymer beads

Experiments were carried first on a system of closely packed polystyrene spheres (9.1 μm in diameter) immersed in water. This model porous sample has two main advantages. First, provided that optimum stacking is achieved, the perfectly spherical shape and the small size distribution (<15% of dispersion) of particles produces a geometrically well defined opened porosity (Fig. 1). Secondly, as revealed by the relatively sharp $^1$H line ( ≈14 Hz at half height using a high resolution 5 mm probe), magnetic susceptibility differences at the liquid/polymer interface are weak producing very low internal gradients within the system. This system was therefore found suitable for calibrating NMR methods and setting the best experimental conditions, i.e., the gradient intensity range, the pulse length and shape, and the duration of the diffusion interval. The PFGSTE_BP sequence was used first to obtain the diffusion attenuation curves. Experimental results obtained for a series of Δ values are shown in Fig. 2a. While the shape is approximately Gaussian below $q = 0.06\ \mu m^{-1}$, an oscillation behaviour is clearly seen at higher $q$ values and remarkably exhibits two maxima at $q = 0.12$ and $q = 0.20\ \mu m^{-1}$. Experiments were perfectly reproducible and led to the same location for these singularities whatever the diffusion interval Δ. While a Gaussian free diffusion behaviour should be observed at very low Δ values, in the present case a slight deviation from this simple regime is already visible at the lowest available diffusion time $\Delta = 10$ ms. Actually during this time interval, the mean square displacement of molecules (an estimation of which can be calculated, with the assumption of a Gaussian distribution of displacements, using the simple equation $\bar{r} = \sqrt{6D_0\Delta}$ with $D_0$ $1.9\ 10^{-9}\ m^2\ s^{-1}$ at

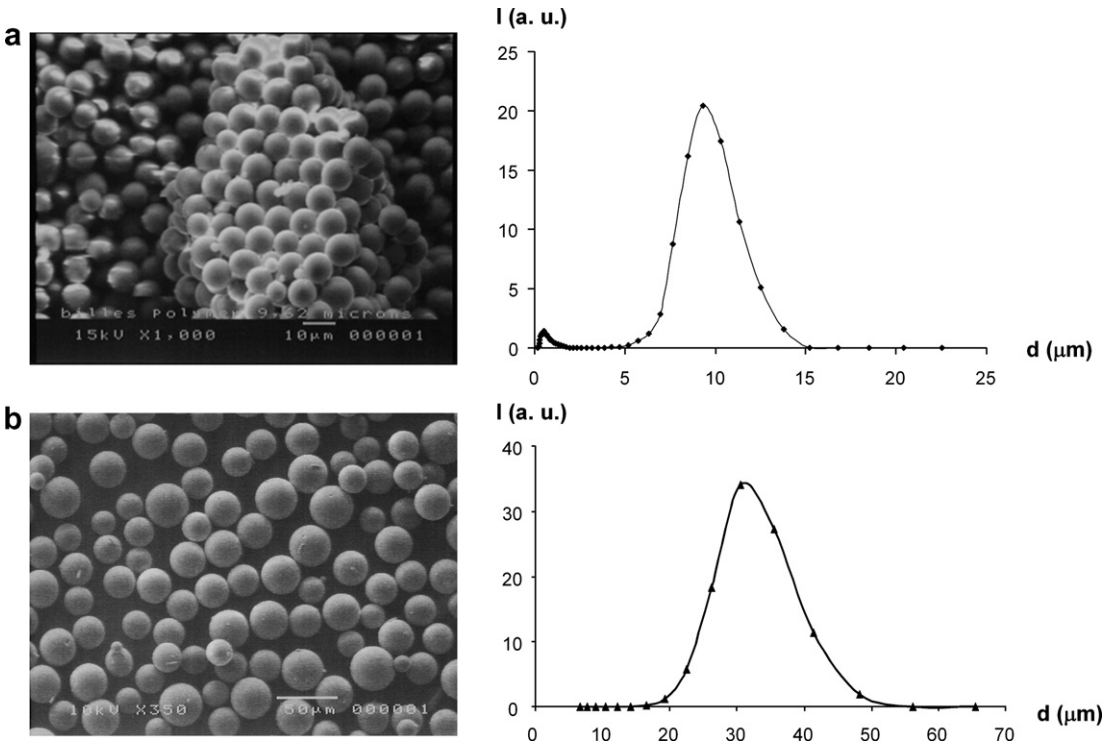


Fig. 1. (Left) Scanning Emission Microscopy (SEM) and (Right) particle size distribution obtained from laser diffraction measurements of (a) polymer spheres and (b) glass spheres samples. In the case of polymer spheres, a weak population of small particles (centered near 0.5 µm) is detected and considered as a negligible fraction of the whole sample.

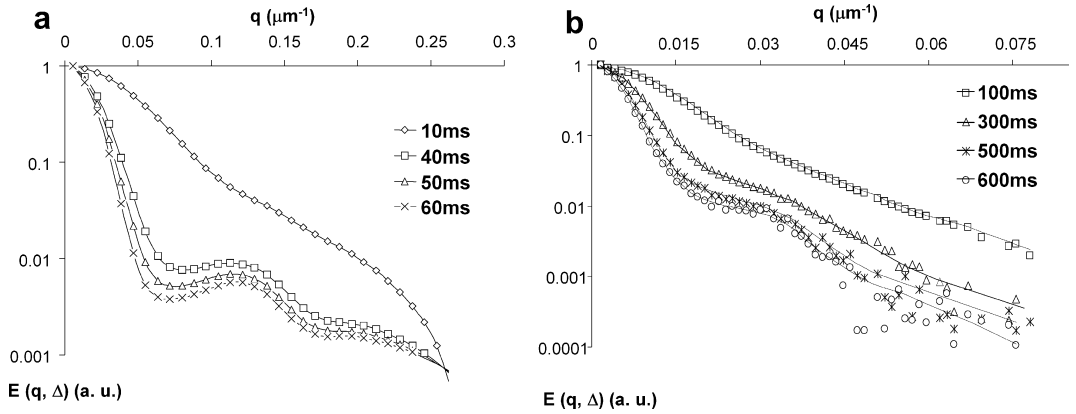


Fig. 2. Diffusion curves at 19 °C and 9.4 T for different values of the diffusion interval Δ. (a) Obtained on polymer beads embedded with water for $\Delta = 10$ ms (empty lozenges, solid line); $\Delta = 40$ ms (empty squares, solid line); $\Delta = 50$ ms (empty triangles, solid line); $\Delta = 60$ ms (crosses, solid line). For all curves, $\delta = 6$ ms. The gradient strength was incremented from 1.96 up to 91.7 G cm$^{-1}$. (b) Obtained on glass beads embedded with water for $\Delta = 100$ ms (empty squares, solid line); $\Delta = 300$ ms (empty triangles, solid line); $\Delta = 500$ ms (crosses, solid line); $\Delta = 600$ ms (empty circles, solid line). For all curves, $\delta = 2$ ms. The gradient strength was incremented from 1.96 up to 91.7 G cm$^{-1}$. Solid lines have been drawn for visualization purpose.

290 K) is in the same order as the size of polystyrene spheres ($\approx 10$ µm). Then, as expected from the theory of the "diffusive diffraction" [7], the amplitude of the oscillation increases with Δ and is attributed to an increased number of jumps between pores. It must be emphasized that, for the first time, the second diffraction peak (located near twice the value of the first maximum in the *q-space*) is experimentally observed in such a porous system. This is produced by molecules which have made at least two different jumps during the diffusion interval, and such a fine effect can be detected here with favourable experimental conditions: (i) the very high signal/noise ratio (1000) obtained at a field of 9.4 T with 32 scans (ii) the use of a relatively high gradient strength which permits the spin magnetization of most molecules to be encoded within a distance smaller than the characteristic dimensions of the system (localized regime). Such a pattern reveals the high homogeneity of the porous structure (spherical shape, perfect stacking) and the low interference of internal gradients.

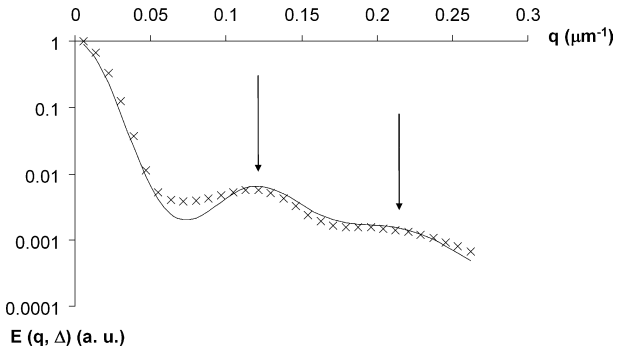


Fig. 3. Diffusion curve obtained on polymer beads (crosses) at 19 °C and $\Delta = 60$ ms compared to the theoretical curve calculated using the "pore hopping model" (solid line) with the following parameters: $a = 2.91$ μm, $b = 9.75$ μm, and $D_{app} = 1.3 \times 10^{-9}$ m$^2$ s$^{-1}$. The $\xi$ value has a negligible influence in that case ($\xi \approx 10\%$).

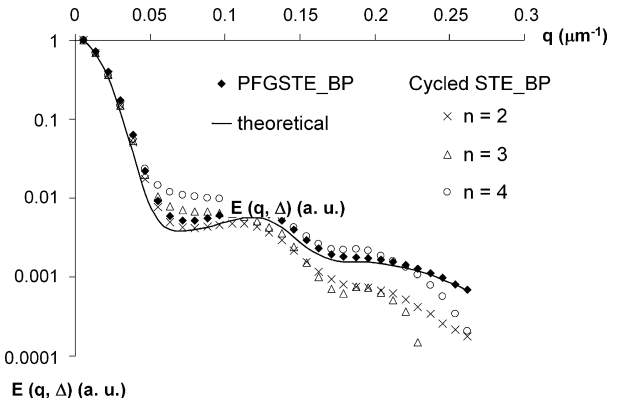


Fig. 4. Diffusion curves obtained at 19 °C and 9.4 T for $\Delta = 50$ ms with the classical PFGSTE_BP sequence (full lozenges) and the cycled STE_BP sequence for $n = 2$ (crosses); $n = 3$ (empty triangle); and $n = 4$ (empty circles). The theoretical curve calculated using the pore hopping model (see Fig. 3) is also given for comparison purpose.

The experimental curve obtained for a diffusion interval $\Delta = 60$ ms was fitted using the pore hopping model formalism [11] developed for the so called Pore Glass system (Fig. 3):

$$E(q,\Delta) = |S_0(q)|^2 F(q,\Delta) = \left|\frac{\sin(\pi q a)}{\pi q a}\right|^2 \times \exp\left[-\frac{6D_{app}\Delta}{b^2 + 3\xi^2} \times \left(1 - \exp(-2\pi^2 q^2 \xi^2)\right)\frac{\sin(2\pi q b)}{2\pi q b}\right] \quad (1)$$

where $S_0(q)$ is the structure factor of a single pore while $F(q,\Delta)$ is relative to the motion of spins between the pores. In this equation, the apparent diffusion coefficient $D_{app}$ essentially monitors the initial Gaussian part of the curve, $a$ which corresponds to the mean pore size acts as a shape factor for the envelope of the signal (whenever $a < b$), whereas $b$ which is defined as the mean pore-to-pore distance is responsible for the location of maxima and minima in the diffraction pattern. As seen in Fig. 3, a good agreement could be obtained using this formalism with the following parameters $a = 2.91$ μm, $b = 9.75$ μm and $D_{app} = 1.3 \times 10^{-9}$ m$^2$ s$^{-1}$. The $\xi$ value which accounts for the structural disorder essentially monitors the line width of the diffraction peak. It has a negligible influence in that case ($\xi \approx 0.1\ b$, i.e., 10%). The $b$ value determined here by NMR diffusion measurements is in close agreement with the mean particle diameter determined by laser diffraction, showing the packing compactness of polystyrene spheres. It is worth noticing that the ratio $b/a$ found here (3.3) is close to that found by Callaghan et al. (2.9) for the similar system of polymer spheres of 16 μm in diameter [12].

The diffusion data acquired using the cycled STE_BP experiment of Latour et al. with $n = 2$, 3, and 4 and the normal PFGSTE_BP sequence are shown in Fig. 4 for $\Delta = 50$ ms. Dealing with polystyrene spheres, almost no magnetic susceptibility differences have to be compensated for. As a consequence no improvement of data is expected using this sequence with increasing $n$ values, instead of the normal PFGSTE_BP sequence. It can be seen that, except a small intensity shift, the same shape is obtained for the four experiments, with identical maxima location in the *q-space* independently of the number of cycles. Only a slight attenuation of the first oscillation can be noticed for $n = 4$ certainly resulting from radiofrequency pulse imperfections or from the use of too short gradient pulses (with regard to rise and fall times).

The diffusive diffraction is also evidenced with the $B_1$ gradient method (Fig. 5a), but apparent differences can be noticed in comparison with $B_0$ gradient data. First, due to the gradient calibration and the smaller range of available gradient strength (4–25 G cm$^{-1}$), longer pulses (up to 30 ms) were needed to access the same range in the $q$-space. As a consequence, part of the initial decay is lost at low values of $q$ because a minimum gradient strength is necessary for a complete defocusing of the nuclear magnetization. This leads to a diffraction peak which is apparently more intense than expected and seen with classical $B_0$ gradient. Second, it can be noticed that the diffraction peak occurs at a slightly different position ($q.b = 1.2$). It has been shown [19] that the violation of the Short Gradient Pulse approximation (SGP), due to the use of long gradient pulses, can be responsible for such a deviation. But other possible causes of discrepancy could simply be of technical nature and related to the inevitable droop of the radio-frequency power amplifier (the second gradient pulse is not exactly of the same amplitude as the first gradient pulse) or just a small difference in sphere packing.

### 2.2. Effect of size poly-dispersity on the diffusive diffraction pattern

In practical cases, the observation of the diffraction pattern is generally hampered by the heterogeneity of the porous structure [7] : a pore size distribution implies a loss of structural periodicity, allowing diffusing molecules to visit pores with different geometries. In such a situation, one

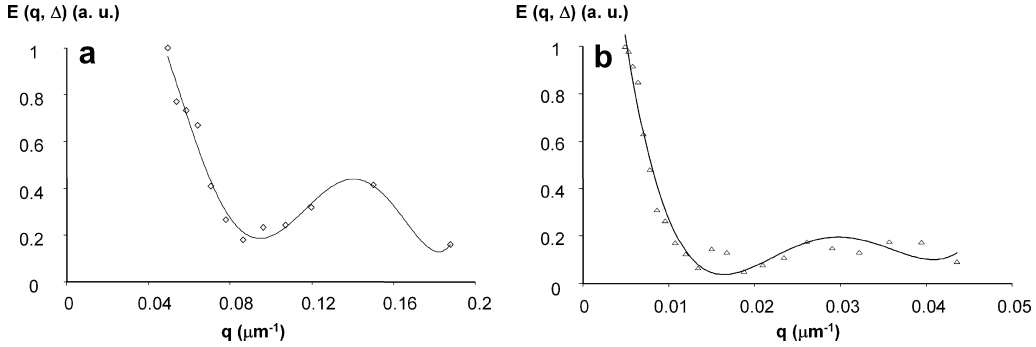


Fig. 5. Diffusion curves obtained at 25 °C and 7.05 T by the $B_1$ method. (a) On the polystyrene beads embedded with water for $\Delta = 50$ ms and $\delta = 30$ ms (empty lozenges). (b) On the glass beads embedded with water for $\Delta = 400$ ms and $\delta = 3$ ms (empty triangles). The accuracy of the data is slightly altered due to technical limitations associated with the high power output of the rf amplifier. Solid lines have been drawn for visualization purpose.

can expect a spreading of the singularities in the *q-space* leading to an attenuation of the diffraction oscillations. The model porous systems of packed sphere particles offers the opportunity of providing a direct experimental proof of this effect as the sample heterogeneity can be intuitively related, in that case, to the size dispersion of the spheres. In other words, while a maximum diffraction effect is expected for strictly mono-sized particles it should be gradually damped with increasing poly-dispersity. This is exactly what has been observed (Fig. 6) when comparing the first sample of polystyrene spheres (dispersion $\sigma < 15\%$) with another sample with a higher poly-dispersity ($\sigma \approx 24\%$) and centered on a slightly different mean diameter value $d = 12$ μm. As seen in Fig. 6 the amplitude of the first diffraction peak is lower and an attenuation of the second peak is observed for the second sample. These observations are confirmed from a Fourier transform in the *r-space* of displacements where the signal intensity is a measure of the molecular displacement probability $\rho(r)$ (Fig. 7). Using this representation, the linewidth at half height of the diffraction peak can be interpreted as a measure of the pore to pore distance distribution [7]. It is obvious from a graphical evaluation (which must be seen as a first approximation) that a higher linewidth is experimentally obtained for the more poly-disperse sample. Moreover the ratio between both measurements ($14/9 = 1.5$) is in close agreement with the ratio of size poly-dispersity ($5.5/4 = 1.4$) determined from laser diffraction (corresponding curves also included in Fig. 7). These results represent a clear experimental demonstration of the specific influence of structural heterogeneity on the observation of the diffusive diffraction pattern at high $q$ values. It is shown that this relationship can be exploited to access the structural disorder in a porous material. The slight deviation of the maxima location in comparison with those deduced directly in the *q-space* representation is imputable to an artefact inherent to the numerical Fourier transformation due to truncated data.

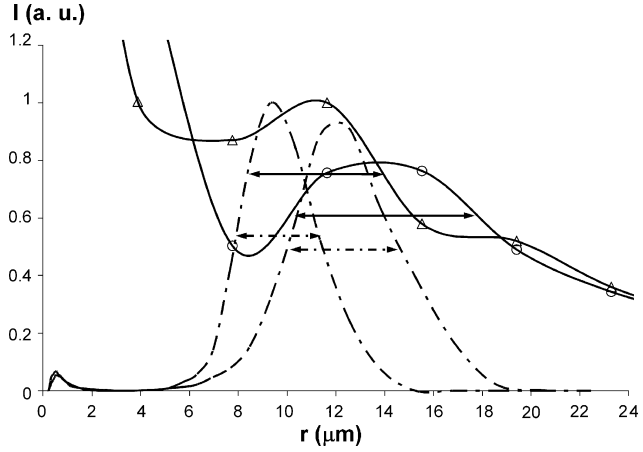


Fig. 7. Fourier transform of the 128 points NMR diffusion curves for the first fraction and the second fraction (solid lines) together with the corresponding graphs of the size distribution obtained on these two systems by laser diffraction (dashed lines). The linewidth of the NMR diffraction peaks and the laser diffraction curves are indicated by arrows.

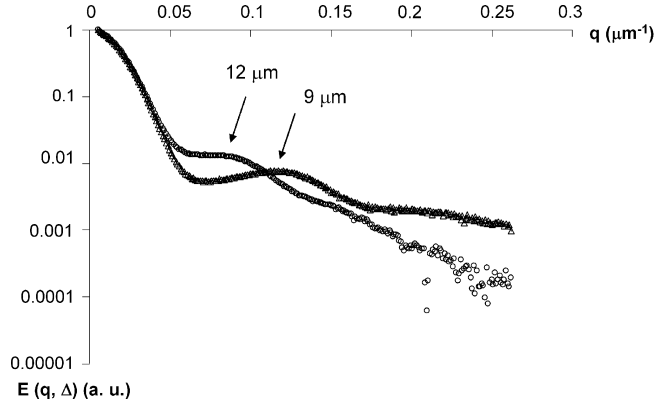


Fig. 6. The 128 points diffusion curves obtained with the PFGSTE_BP sequence with $\Delta = 50$ ms, $\delta = 6$ ms for two samples of polystyrene spheres bearing two different polydispersities: a dispersion $\sigma < 15\%$ for the first fraction (empty triangles) and a dispersion $\sigma \approx 24\%$ for the second fraction (empty circles). The amplitude of the diffraction oscillation is shown to be higher for the first sample involving the lowest polydispersity.

### 2.3. Glass beads systems

A second difficulty that limits the observation of the diffusive diffraction effect in a porous material is the presence

of magnetic local field gradients (background gradients) due to the susceptibility differences at the liquid/solid interfaces. In order to evaluate the influence of these local gradients and the efficiency of the different NMR sequences, we investigated another granular system of glass spheres 31 μm in diameter with a highly spherical shape and a controlled size poly-dispersity (18%) (Fig. 1b). Actually, silica glass has a magnetic susceptibility which strongly differs from water as revealed by the large linewidth of 2500 Hz measured on the embedded system at 9.4 T. In such conditions the basic STE sequence cannot be used to monitor the molecular translational diffusion because the major part of the signal is lost before acquisition. This is due to the dephasing of the nuclear spin magnetization produced by the strong internal gradients experienced during the few milliseconds of application of the gradient pulses. In the bipolar version of the Pulsed Field Gradient Stimulated Echo sequence [16], the single gradient pulse for encoding and decoding periods is replaced by a cluster of two bipolar pulses separated by a π pulse. This inversion pulse refocuses the dephasing due to background gradients while the dephasing due to applied gradients is maintained because of the inversion of the gradient polarity.

Experimental diffusion decays, measured using the PFGSTE_BP sequence, are shown in Fig. 2b. As the mean sphere diameter is three times higher than the polystyrene spheres a narrow range of $q$ values (i.e., shorter gradient pulses of 2–3 ms) and longer diffusion times Δ were required to observe the diffraction peaks. A similar shape was obtained for different Δ values with a bump at $q \approx 0.03\ \mu m^{-1}$ which corresponds to a parameter $b = 33$ μm, in close agreement with the mean particle size determined from laser diffraction measurements. The amplitude of the oscillation is strongly attenuated in comparison with the polystyrene sample and the second peak is not visible near $q.b = 2$. Both can be attributed to the cumulative effect of local field gradients and the higher structural heterogeneity in this system.

In the PFGSTE_BP sequence, the refocusing process to be complete requires that the same background gradients are experienced during the application of the two bipolar pulses. In practice, molecules can move significantly during this time interval, and the smaller the pulses, the better the refocusing process is. A first possibility to reduce the pulse length is to increase the magnetic field gradient strength. In the cycled PFGSTE_BP sequence proposed by Latour et al. the bipolar pulse is replaced by a train of $(n + 1)$ π pulses separating by $2n$ shorter gradient pulses of alternating sign. They initially used this sequence to measure diffusion coefficients in the presence of strong magnetic local field gradients. We evaluated here the ability of this method to observe, in such a situation, the diffusive diffraction phenomenon in porous media. Using the sequence with $n = 2$ and the same durations for the total gradient pulse length $\delta$ and the diffusion interval Δ, the second diffraction peak near $q.b = 2$ could be observed (Fig. 8). The total diffusion curve including the two peaks was also fitted according to

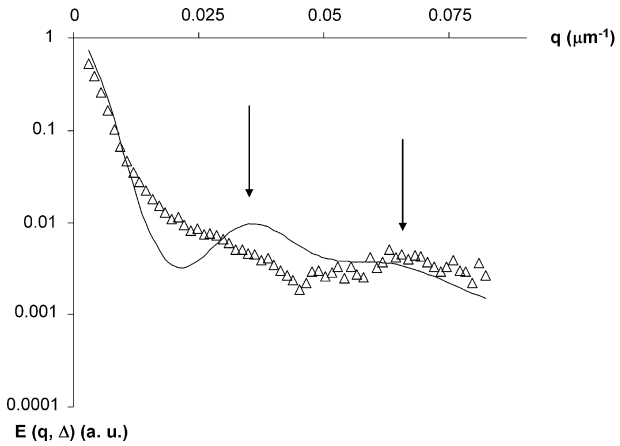


Fig. 8. Diffusion curve obtained on glass beads (empty triangle) at 19 °C and Δ = 200 ms compared to the theoretical curve calculated using the "Pore Hopping Model" (solid line) with the following parameters: $a = 33$ μm, $b = 8$ μm, $D_{app} = 1.8 \times 10^{-9}\ m^2\ s^{-1}$, and $\xi \approx 15\%$.

Eq. (1). Although the theoretical curve could not fit accurately the experimental curve, maxima and minima locations could match and led to a $b$ value slightly higher than the particle diameter (33 μm) measured from laser diffraction measurements. Possible reasons for this discrepancy could be the remaining influence of background gradients and the higher complexity of the system. A bump also appears using the method based on gradient of the radiofrequency field $B_1$ (Fig. 5b); This was quite expected because this method is known to be immune to internal gradients associated with the static magnetic field. Again, because of the higher dimensions of the system, narrower gradient pulses could be used (near 3 ms) to scan the required q space and lead this time to $a$ $b$ value of 33 μm, in agreement with other methods and with the system characteristic dimensions.

### 2.4. Comparison with a real porous system

We have recently reported the experimental observation of the diffusive diffraction phenomenon on a real porous material (a cross-linked polystyrene synthesized by an inverse emulsion process) using the radiofrequency field $B_1$ method. The diffusion attenuation obtained at 10 ms and the fitted theoretical curve calculated with Eq. (1) are shown in Fig. 9. The $b$ value determined here (20.2 μm) using the pore hopping model formalism is similar to the previous one (19 μm) initially determined from a signal decomposition in two Gaussian curves (a first half Gaussian component to account for the normal diffusion decay and a second Gaussian component centred at a non zero $q$ value to account for hopping) [15].

As opposed to the model systems of packed spheres, the effect was observed only at short values of the diffusion time Δ, i.e., at a time interval high enough to make exclusively one jump between two pores. After that, the diffraction pattern rapidly disappears as Δ increases. This is due

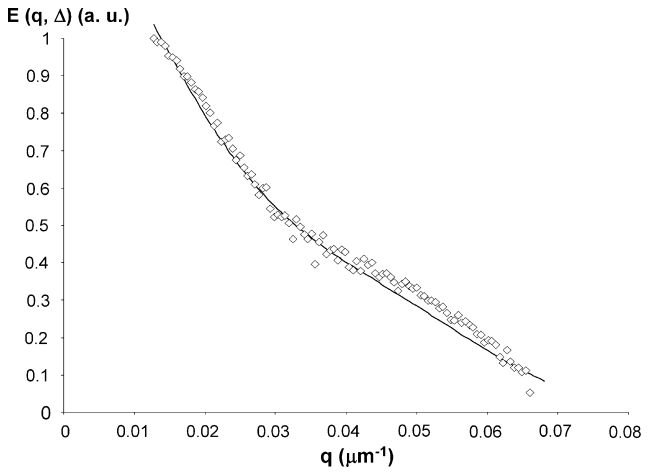


Fig. 9. The 128 points diffusion curve (empty lozenges) obtained on a real porous material (a cross-linked polystyrene synthesized by an inverse emulsion process) using the radiofrequency field $B_1$ method for $\Delta = 14$ ms and $\delta = 5$ ms compared to the theoretical curve calculated using the "Pore Hopping Model" (solid line) with the following parameters: $a = 10.2$ μm, $b = 9.9$ μm, $D_{app} = 2.01 \times 10^{-9}$ m$^2$ s$^{-1}$, and $\xi \approx 25\%$.

to the more complex structure of this material which produces a high pore size distribution, complex cavity shapes and connections. Another effect, which is a direct consequence of this structural disorder, is the highly non uniform distribution of local magnetic field gradients with intensity and direction rapidly changing within very short distances. Thus, while a diffractive effect could be observed using the $B_0$ gradient methods in the case of the glass spheres system (which however contained apparently stronger magnetic field gradients—$^1$H linewidth of 2500 and 400 Hz for the polymer at 9.4 T), attempts to obtain similar results here completely failed and always gave normal Gaussian attenuations, even using the cycled STE_BP sequence. This result shows that during the application of gradient pulses, although short, nuclear spins can experience highly different background gradients inside the same cavity and this results in an incomplete refocusing process by the π pulse involved in the bipolar gradient sequence. The subsequent modification of the diffusion signal in the *q-space* representation is certainly a complex process. However, it can be understood intuitively as a spreading of the diffraction peaks at high q values, leading to an apparent decay instead of the diffraction peak. This decay being slower than the normal diffusion decay, it can lead to an underestimation of the diffusion coefficients deduced from a Gaussian fit to experimental data. Such effects do not affect diffusion data obtained with $B_1$ gradients as this method is totally immune to any influence of internal gradients of the static magnetic field [15].

## 3. Conclusion

In this paper, the diffusive diffraction phenomenon has been investigated by diffusion measurements performed on model systems of closely packed sphere particles embedded with water. Using first quasi mono-disperse polystyrene spheres, the diffraction effect was finely observed in close agreement with the pore hopping model theory. In addition to the first oscillation at $q.b = 1$, a second diffraction peak at $q.b = 2$ could be clearly detected for the first time in such systems, revealing molecules experiencing two consecutive jumps between pores during the diffusion interval. The use of a rational selection of different samples chosen according to their size poly-dispersity and magnetic susceptibility enabled us to determine the specific effect of structural disorder and internal magnetic fields. From this basis, we evaluated the ability of different sequences (the PFGSTE_BP, the cycled STE_BP and the $B_1$ gradient method) to observe the diffraction pattern. Applied to a real porous polymer material the diffraction effect could be observed only by the methods using $B_1$ gradients and not with $B_0$ gradients. It is shown that this is due to the highly hetereogeneous structure of this system at a very small length scale leading to rapidly changing background gradients within very short distances.

## 4. Experimental section

All experiments based on static magnetic field gradients were carried at 9.4 T on a Bruker Wide Bore spectrometer (proton resonance frequency of 400.13 MHz) at 290 K. We used a standard Bruker micro 2.5 imaging system capable of delivering a maximum gradient strength of 100 G cm$^{-1}$ in each three directions. The probe was equipped with a bird cage coil (10 mm in diameter) and the 90° pulse was adjusted to 10.5 μs. Diffusion measurements were performed using the 11 intervals and the cycled version of the PFGSTE_BP sequence [17]. The Pulse field gradient length $\delta$ was set to values in the range 3–6 ms and the diffusion time $\Delta$ was varied between 10 and 500 ms. $\delta$ was kept constant for the whole series of measurements performed for different diffusion times $\Delta$ and concerning a given sample. The *q-space* encoding was achieved by incrementing linearly the gradient amplitude between 2% and 95% in 32 steps. In the cycled PFGSTE_BP sequence the encoding and decoding steps are composed of a series of $(n + 1)$ π pulses separated by $2n$ gradient pulses of alternative sign. We used a number of cycles $n$ of 2, 3, and 4 which corresponds to elementary pulsed field gradient lengths $\delta/2n$ of 1500, 1000, and 750 μs. Experiments using the radiofrequency field gradient ($B_1$ gradient) were performed at 7.05 T on a Bruker Wide Bore spectrometer (proton resonance frequency of 300.15 MHz) at 298 K. The magnet was equipped with a home-made probe where a uniform RF gradient up to 25 G cm$^{-1}$ is produced by a two-turn flat coil orthogonal to the standard saddle shaped coil; the latter is used at the receiving stage or for generating pulses of homogeneous rf field. The electrical orthogonality of the two coil systems is finely adjusted by slightly reorienting the flat coil with respect to the saddle coil so as to minimize their leakage. We

used $\delta$ values in the range of 5–30 ms and a diffusion time $\Delta$ between 50 and 400 ms. The gradient amplitude was incremented regularly between 15% and 88% of its maximum amplitude in 20 steps. This is achieved by the linear property of the RF power amplifier. The first value of the gradient is not zero because a full magnetization dephasing must be reached whatever the gradient value.

The gradient strength was calibrated in both cases with water and octanol.

Calibrated polystyrene spheres were purchased from Merck S.A. (9.1 μm, <15% of dispersion and 12 μm, ≈ 24% of dispersion). Glass spheres were provided by Malvern S.A. (31 μm, about 18% of dispersion). The mean square diameter and poly-dispersity were systematically controlled in our laboratory by laser diffraction before analysis. Samples were first washed three times and filled with deionised water or acetone of p.a. quality purchased from Merck. The spheres were then introduced in standard NMR tubes (inner diameter of 9 and 3 mm for measurements at 400 and 300 MHz, respectively) and centrifuged during 20 min to achieve random loose packing.

## Acknowledgment

Part of this work was supported by the ANR Grant Blan06-2_139020 ("Instrumentation in Magnetic resonance" Project).

## References

[1] P.T. Callaghan, NMR imaging, NMR diffraction and applications of pulsed gradient spin echoes in porous media, Magn. Reson. Imaging 14 (1996) 701–709.
[2] D.J. Woessner, NMR SPIN-ECHO self-diffusion measurements on fluids undergoing restricted diffusion, J. Phys. Chem. 67 (1963) 1365.
[3] E.O. Stejskal, E. Tanner, Spin diffusion measurements: spin echoes in the presence of a time-dependent field gradient, J. Chem. Phys. 42 (1965) 288–292.
[4] P.N. Sen, Time-dependent diffusion coefficient as a probe of geometry, Concept Magn. Reson. Part A 23A (2004) 1–21.
[5] J.G. Seland, M. Ottaviani, B. Hafskjold, A PFG-NMR study of restricted diffusion in heterogeneous polymer particles, J. Colloid Interf. Sci. 239 (2001) 168–177.
[6] P.P. Mitra, P.N. Sen, L.M. Schwartz, P. Le Doussal, Diffusion propagator as a probe of the structure of porous media, Phys. Rev. Lett. 68 (1992) 3555.
[7] P.T. Callaghan, Principle of Nuclear Magnetic Resonance Microscopy, Oxford Science Publications, New York, 1991.
[8] A. Coy, P.T. Callaghan, Pulsed gradient spin echo nuclear magnetic resonance for molecules diffusing between partially reflecting rectangular barriers, J. Chem. Phys. 101 (1994) 4599.
[9] S.J. Gibbs, Observations of diffusive diffraction in a cylindrical pore by PFG NMR, J. Magn. Reson. 124 (1997) 223–226.
[10] S.L. Codd, P.T. Callaghan, Spin echo analysis of restricted diffusion under generalized gradient waveforms: plznzr, cylindrical, and spherical pores with wall relaxivity, J. Magn. Reson. 137 (1999) 358–372.
[11] P.T. Callaghan, A. Coy, T.P.J. Halpin, D. MacGowan, K.J. Packer, F.O. Zelaya, Diffusion in porous systems and the influence of pore morphology in pulsed gradient spin-echo nuclear magnetic resonance studies, J. Chem. Phys. 97 (1992) 651–662.
[12] P.T. Callaghan, A. Coy, D. MacGowan, K.J. Packer, F.O. Zelaya, Diffraction-like effects in NMR diffusion studies of fluids in porous solids, Nature 351 (1991) 467.
[13] D. Topgaard, C. Malmborg, O. Söderman, Restricted self-diffusion of water in a highly concentrated W/O emulsion studied using modulated gradient spin-echo NMR, J. Magn. Reson. 156 (2002) 195–201.
[14] A.M. Torres, R.J. Michniewicz, B.E. Chapman, G.A.R. Young, P. Küchel, Characterisation of erythrocyte shapes and sizes by NMR diffusion-diffraction of water: correlations with electron micrographs, Magn. Reson. Imaging 16 (1998) 423–434.
[15] J.F. Kuntz, G. Trausch, P. Palmas, P. Mutzenhardt, D. Canet, Diffusive diffraction phenomenon in a porous polymer material observed by NMR using radio-frequency field gradients, J. Chem. Phys. (2007) 134904.
[16] R.L. Karlieck, I.J. Lowe, A modified pulsed gradient technique for measuring diffusion in the presence of large background gradients, J. Magn. Reson. 37 (1980) 75–91.
[17] L.L. Latour, L. Li, C.H. Sotak, Improved PFG stimulated-echo method for the measurement of diffusion in inhomogeneous fields, J. Magn. Reson. Ser. B 101 (1993) 72–77.
[18] D. Canet, radiofrequency field gradient experiments, Prog. Nucl. Magn. Reson. Spec. 19 (1997) 1.
[19] L. Avram, Y. Assaf, Y.J. Cohen, The effect of rotational angle and experimental parameters on the diffraction patterns and micro-structural information obtained from q-space diffusion NMR: implication for diffusion in white matter fibers, J. Magn. Reson. 169 (2004) 30–38.